From electromagnetically induced transparency to absorption in planar optical metamaterials

Bo Na (那 波)[1], Jinhui Shi (史金辉)[1,2*], Chunying Guan (关春颖)[1], and Zhengping Wang (王政平)[1]

[1] *Key Laboratory of In-Fiber Integrated Optics of Ministry of Education, College of Science, Harbin Engineering University, Harbin 150001, China*

[2] *State Key Laboratory of Millimeter Waves, Southeast University, Nanjing 210096, China*

[*] *Corresponding author: hrbeusjh@gmail.com*

Received July 23, 2013; accepted September 25, 2013; posted online November 4, 2013

We theoretically investigate the classical analog of electromagnetically induced transparency (EIT) and electromagnetically induced absorption (EIA) in a planar metamaterial at optical frequency, which originates from destructive and constructive interference between dark and radiative elements. The metamaterial consists of two coupled resonators with different geometries. An EIT-like transparent window with low absorption is observed and found to be strongly affected by resonant states of the resonators. The transition between the EIT and EIA is achieved by changing the split width and coupling distance. The absorption is enhanced up to 2.5 times compared with the dipolar case. The excitation of the dark mode is very important for EIT- and EIA-like responses of the proposed metamaterial. The EIT and EIA phenomena offer a potential method for manipulating electromagnetic response in metamaterial-based devices.

OCIS codes: 160.3918, 260.2110, 260.5740.
doi: 10.3788/COL201311.111602.

In the past decade, metamaterials have attracted considerable attention because of their various unique electromagnetic responses that are not usually found in natural materials[1]. Metamaterials can achieve the desired electromagnetic effects by appropriately designed structural elements of subwavelength sizes. Numerous functionalities and devices have been realized based on planar and three-dimensional metamaterials[1,2]. Given their easy fabrication, planar metamaterials (also called metasurfaces) have been extensively investigated to realize negative dielectric permittivity[3], asymmetric transmission[4−6], focusing of electromagnetic waves[7], optical activity, and circular dichroism[8,9]. Metasurfaces with designed phase discontinuities have recently led to anomalous reflection and refraction phenomena[10,11] and photonic spin Hall effect[12]. Considering the growing interest in terahertz science, the design and fabrication of metamaterials for manipulating terahertz wave propagation have also been extensively investigated[9,11,13−23]. Planar metamaterials have been demonstrated to reveal classical analogs of quantum phenomena, including electromagnetically induced transparency (EIT)[24−37] and Fano resonance[38−48]. The EIT phenomenon renders an initially opaque medium transparent over a narrow spectral range within an absorption line because of the destructive interferences between two different excitation pathways. The coupling effects of subwavelength resonators in metamaterials can be regarded as counterparts of state transitions in quantum systems. For instance, asymmetric coupling between two bright modes can excite a high-Q EIT-like mode formed by counterpropagating currents (i.e., a so-called trapped mode resonance that is associated with an asymmetric Fano-type line shape)[24]. The EIT phenomenon has many potential applications, such as in the production of slow light and enhancement of light-matter interaction.

Metamaterial analogs of electromagnetically induced absorption (EIA) have been reported in recent publications[49-52]. The EIA phenomenon can be also understood in terms of destructive interference between the radiative and dark modes; hence, it refers to enhancing absorption. The EIA-like phenomena are produced by a retardation-induced phase shift in a bilayered metamaterial[49] or different phases of two resonators coupled to an external wave[50]. The transition between EIT and EIA can be easily obtained by controlling the damping of the radiative (R) and dark (D) resonators or the coupling mechanism in metamaterials[51]. In the microwave range, metamaterials with a branch with side-coupled SRRs are utilized to describe the absorption, EIT, and EIA in two-, three- and four-level atomic systems[52]. However, the classical analog of the EIA effect in single-layer photonic metamaterials remains unclear. The photonic metamaterial analog of the EIA effect has great potential for nonlinear, switching, and sensing applications, especially for harvesting solar light. Therefore, the realization of the EIA phenomenon in a single-layered photonic metamaterial is highly desirable because it can be easily fabricated.

In this letter, we investigate classical analogs of the EIT and EIA phenomena in a single-layer planar metamaterial consisting of an array of two coupled resonators at optical frequency range. The coupling of a radiative (low-Q) mode and a dark (high-Q) mode leads to an EIT-like transmission with a Fano-type asymmetric line shape because of destructive interference in the far-field. Detuning is easily controlled by adjusting the width of the split in one resonator. The formation of the EIT and EIA effects strongly depends on the interaction between two resonators with different sizes. In addition to observing enhanced transmission in the EIT case, the near-field coupling of the bright mode to the dark mode results in a narrow peak with enhanced absorbance on top of the broad dipolar absorbance feature. The EIT and EIA

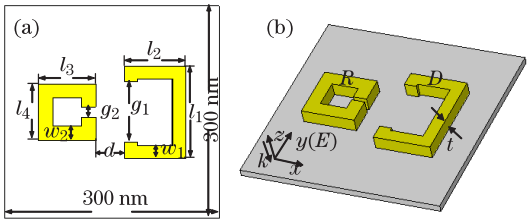

Fig. 1. The planar metamaterial. (a) Front view of a unit cell and (b) the stereogram of a unit cell. l_1, l_2, l_3, l_4, w_1, w_2, and t are considered to be 130, 85, 80, 80, 18, 20, and 20 nm, respectively. g_1, g_2, and d are variables. R and D denote the radiative and dark resonators, respectively. A plane wave is incident along the -z direction, with $\boldsymbol{H}$ and $\boldsymbol{E}$ along the x and y directions.

effects offer an opportunity to design photonic metamaterials and tailor optical properties in plasmonic nanostructures.

The single-layer metamaterial with a broken structural symmetry exhibits a trapped-mode resonance when the electric field of the incident wave is perpendicular to the mirror line of the asymmetrically split rings. Such sharp resonance can be regarded as a Fano resonance with an asymmetric line shape that can be described by a Fano-type model[28]. This electromagnetic mode is weakly coupled to free space. Hence, most electromagnetic energy is trapped near the meta-surface. The electromagnetic response of the metamaterial is well-tailored to achieve classical analogs of the EIT and EIA phenomena. The schematic of our metamaterial is presented in Fig. 1. A front view and a stereogram of a unit cell of a metamaterial are shown in Figs. 1(a) and (b), respectively. The unit cell is composed of two gold split ring resonators (SRRs) with different sizes, and the splits of the two rings are placed face to face. The unit cell is arranged in a periodic array with a period of 300 nm in both the x and y directions. The detailed structural parameters are shown in Fig. 1. The geometrical parameters of the asymmetrical split rings are denoted by l_1, l_2, l_3, l_4, w_1, w_2, g_1, g_2, d, and t. In the simulations, l_1, l_2, l_3, l_4, w_1, and w_2 are assumed to be 130, 85, 80, 80, 18, and 20 nm, respectively. Parameters g_1 and g_2 denote the corresponding split widths of the two resonators. Parameter d represents the distance between two elements that is used to control the coupling strength. Parameters g_1, g_2, and d are variable in the following discussion. The metallic asymmetrical split rings have a thickness of t=20 nm embedded in the air in the calculations, given that the influence of the dielectric substrate is negligible[25,53]. The large and small asymmetrical split ring resonators serve as dark and radiative oscillators, marked by "D" and "R" in Fig. 1(b). The system can be understood by a simple two-oscillator EIT model[51].

$$\omega_{\rm r}^{-2}\,\ddot{p}(t)+\gamma_{\rm r}\omega_{\rm r}^{-1}\,\dot{p}(t)+p(t)=f(t)-\kappa q(t),$$
$$\omega_{\rm d}^{-2}\,\ddot{q}(t)+\gamma_{\rm d}\omega_{\rm d}^{-1}\,\dot{q}(t)+q(t)=-\kappa p(t). \quad (1)$$

The radiative resonators $p(t)$ and dark resonators $q(t)$ are described by resonance frequency ω_r, ω_d, and damping factor γ_r, γ_d. The R resonator can be driven by an external field $f(t)$. κ describes the coupling strength between the R and D resonators. The permittivity of gold ε_m is described by the Drude model[28], in which the plasma and collision frequencies are $\omega_p = 1.374\times10^{16}$ rad/s and $\upsilon_c = 4.08\times10^{13}$ Hz, respectively. The electromagnetic responses of the planar metamaterial are numerically investigated through a commercial finite-integration package, CST Microwave Studio. To mimic an infinite array, we use the periodic boundary condition along the x and y axes.

The simulated results of planar metamaterials are completed at normal incidence in the 400 to 600 THz frequency range, where the electric field is directed along the y axis (Fig. 1). The dependence of transmission, reflection, and absorption spectra of the metamaterial on the split width g_2 of the R resonator is shown in Fig. 2. In the calculations, d=40 nm, g_1=85 nm, and other parameters are kept unchanged. When g_2=4 nm in Fig. 2(a), a transmission peak B forms between the two transmission minima A and C, corresponding to a reflection dip. This resonance with an asymmetric line shape can be regarded as a classical analog of EIT, because this transmission peak occurs in between two absorption peaks and matches the absorption dip shown in Fig. 2(d). The quality factor of the resonance is approximately 19.5, which is calculated from the transmission spectra. Considering that the resonance feature has an asymmetric line shape, we choose the highest peak and the lowest dip on the resonance curve as two extreme points and note the full-width (Δf) at half maximum-bandwidth[44] to obtain the value $Q = f_0/\Delta f$. The absorption can be calculated as A= 1- T - R. When g_2=2 nm in Fig. 2(b), the higher Q factor of 43 is observed because of the small absorption in Fig. 2(e), although the resonance feature is extremely weak. When g_2=0 nm (i.e., the R resonator becomes a closed ring), the EIT-like pass band with

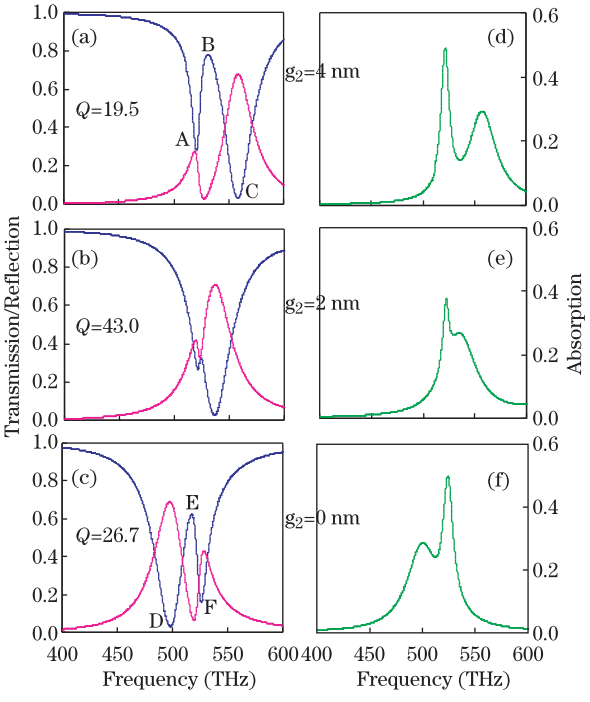

Fig. 2. Spectra of transmission, reflection, and absorption of the metamaterials with d=40 nm, g_1=85 nm for different split widths of g_2=0, 2, 4 nm. Spectra of ((a) to (c)) transmission and reflection and ((d) to (f)) absorption. A to F denote typical resonances.

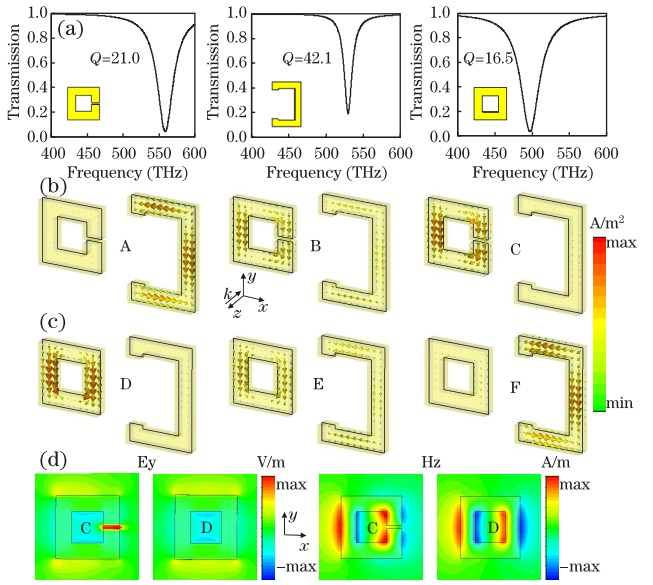

Fig. 3. (a) Transmission spectra of three individual resonators. (b) to (c) Simulated current density distributions at resonances A to F marked in Figs. 2(a) and (c). (d) Field distributions of Ey and Hz at resonances C and D.

Q=26.7 in Fig. 2(c) appears to be considerably similar to that in Fig. 2(a). However, the line shape inversion is clearly seen from two exchanged transmission minima, indicating that the detuning is changed from negative to positive. Firstly, the resonant frequency ω_r of the R resonator is larger than that of the D resonator. The resonance frequency ω_r of the R resonator reveals a redshift, and the D resonator remains nearly unchanged when the split width g_2 is decreased. When ω_r approaches the resonance frequency ω_d of the D resonator, the absorption dip in Fig. 2(e) almost disappears, and the absorption changes into an unusual spectrum with a narrow peak at the resonance frequency $\omega_r = \omega_d$. Afterward, the EIT-like transmission peak E reappears in the case of $\omega_r < \omega_d$, where the R resonator bears no split.

The coupling mechanism in metamaterials has been well examined[54−61]. The metamaterial analog of the EIT phenomenon can be explained as a destructive coupling between so-called "radiative" and "dark" modes that are required to have a significant difference in the quality factors (or line width) and a sufficiently small frequency detuning. The interaction between two distinctive resonances leads to hybridization, thereby causing the EIT-like transmission peak. The simulated transmission spectra of the small SRR with a split of g_2=4 nm, the large SRR, and the closed-ring resonator (CRR) are shown in Fig. 3(a). The corresponding resonant frequencies are approximately 558, 531, and 498.6 THz. Evidently, the three resonant modes have different Q factors of 21, 42.1, and 16.5. The large SRR has a narrow line width with a higher Q-factor, whereas the small SRR shows a broad line width with a lower Q-factor regardless of a split. Therefore, the large and small resonators can be understood as the dark and radiative oscillators, respectively. When two resonators interplay with each other, resonance hybridization occurs. To further understand the coupling mechanism between two elements to achieve EIT in the planar metamaterial, we study the current density distributions of the metamaterials. The current density distributions at the resonances of two cases in Figs. 2(a) and (c) are illustrated in Figs. 3(b) and (c), respectively. The two transmission minima A and C are individually dominated by the large SRR (the D resonator) and small SRR (the R resonator) (Fig. 3(b)). At resonance A, only the large SRR is excited. Two nodes exist around the right-angle corners for the excited current oscillating along the SRR, and the induced current seems to comprise two antiparallel current pairs. Consequently, the scattering field from the middle current cancels the scattering field from the other two currents. This quadrupole-like electromagnetic response resembles a trapped-mode resonance that couples weakly to free space[24]. The high-Q resonance results from excitation of antiparallel current modes. Therefore, the large SRR can be termed as a D resonator. However, at resonance C, only the small SRR is excited, while the large SRR is barely excited. Although the small SRR has a sufficiently narrow split, two parallel currents with almost equal amplitudes oscillate along the two vertical branches, with nodes at the top and bottom arms. Such symmetric current mode forms a dipole radiation with a broad line width. Thus, the small SRR can be regarded as an R resonator. Interference between the D and R resonators can lead to an EIT-like phenomenon. Importantly, the antiparallel y-oriented currents in the R and D resonators can suppress scattered fields and make the metamaterial weakly couple to free space. The EIT-like narrow transmission resonance B originates from hybridization of resonances A and C because of near-field interaction between two simultaneously excited resonators.

In the other case of the metamaterial with CRRs and SRRs, the induced current distributions at the transmission peak E and two transmission minima D and F are shown in Fig. 3(c). The large SRR with a quadrupole-like current distribution still acts as a D resonator, and the CRR with a symmetric current configuration is radiative. Similar to the above discussion, the destructive interference between the SRR and CRR resonators leads to the EIT-like pass band. The presence of the split is clearly observed to strongly affect the resonant frequency ω_r of the R resonator and change the sign of the detuning, although the symmetric current distribution basically remains unchanged. The field distributions of Ey and Hz are presented in Fig. 3(d) to demonstrate the resonant nature of the R resonators. The field maps of Hz at both resonances C and D are similar, with symmetric current modes. However, the electric response Ey at resonance C is considerably stronger than that at resonance D because of charge accumulation across the small gap. More energy is necessary to maintain this violent Ey resonance. Hence, the SRR with a split has a considerably higher resonant frequency than that of the CRR. The geometrical parameters can be used to determine the resonant frequency of the SRR. Along with this, the change of one resonance will modulate interference effects between the D and R resonators. Subsequently, both transmission and absorption spectra are strongly affected. In Fig. 2(e), the absorption spectrum almost becomes a single peak that is distinctively different from the EIT effect.

The EIT phenomenon in a metamaterial renders it

transparent over a narrow spectral range within an absorption band, corresponding to an absorption minimum. The EIT phenomenon can generally be achieved by coupling between a radiative and a dark mode because of destructive interference. The EIA phenomenon refers to enhanced absorption resulting from constructive interference between two radiative and dark modes. The split width and the coupling distance of two resonators can be controlled to achieve a transition from the EIT to EIA effect. Considering the practical availability of the proposed metamaterial, focus will be given to the CRR-SRR metamaterial without the extremely small split, g_2=0 nm.

Firstly, we study role of the D resonator (i.e., the large SRR) in the EIA phenomenon. The effects of the split width g_1 of the D resonator in the metamaterial are mainly investigated. We can only tune the resonant frequency ω_d and damping factor γ_d by changing g_1, while the R resonator is kept unchanged. The dependence of the transmission and absorption of the optical metamaterial on the split width g_1 is illustrated in Figs. 4(a) and (b), in which the distance d between the CRR and SRR remains unchanged, d=40 nm. When g_1=55 nm, the EIT-like effect disappears, and the radiative and dark modes degenerate to share the same frequency at approximately 500 THz. The transmission spectrum only shows a broad transmission stop band with no splitting. Accordingly, a broad dipolar absorption spectrum is observed with a maximum of approximately 21%. When the split width g_1 is larger than 55 nm, the transmission stop band is split, and the metamaterial is characterized by two new modes corresponding to two transmission minima. The transmission peak arises from coupling of the radiative and dark modes. The transmission dip at the high frequency is a little deeper than the transmission dip at low frequency until g_1 is 65 nm. As the split width g_1 is increased, ω_r and γ_r of the radiative mode remain unchanged, while the damping factor γ_d increases, and the resonant frequency ω_d of the dark mode progressively blue-shifts. Therefore, the transmission pass band becomes more pronounced. More interestingly, the broad dipolar absorption is rapidly changed into a narrow peak. When g_1 = 70 nm, the absorption is markedly enhanced up to 50%, and the absorption enhancement factor is approximately 2.5 of the dipolar case. This phenomenon can be regarded as a metamaterial analog of the EIA phenomenon, in which the absorption is enhanced because of constructive interference. As g_1 is increased from 70 to 80 nm, the absorption peak with a maximum of 50% further blue-shifts, but an absorption dip gradually appears, indicating a transition from the EIA to EIT phenomenon. Under specific circumstances, increasing loss of the dark mode leads to enhanced transmission and absorption instead of suppressed absorption because of destructive interference. Based on appropriate design of resonators in single-layer metamaterials, classical analogs of both EIT and EIA phenomena can be achieved to enhance the light-matter interaction and optical nonlinearity.

In addition to the intrinsic properties of the R and D resonators, the coupling strength κ is also a crucial factor for determining the electromagnetic response of a metamaterial. Considering that the distance between two resonators is proportional to the strength of the coupling mechanism, this distance can be used to estimate the coupling strength[51,60,61]. Next, Figs. 4(c) and (d) show the dependence of the transmission and absorption spectra on the coupling strength controlled by the distance d between the CRR and SRR resonators, in which the split width is always g_1=65 nm and other parameters are kept unchanged. Strong coupling leads to a broad transmission pass band, while weak coupling leads to a narrow and sharp transmission pass band. With increasing distance d, the decreasing coupling strength results in a strong excitation of the dark mode, thus more energy dissipates in the dark resonator. The enhanced absorption can be obtained near the resonant frequency $\omega_{\rm d}$ of the dark mode. When d=30 nm, only a transmission dip and a low absorption peak of approximately 25% can be seen in Figs. 4(c) and (d), respectively. As distance d increases, the transparency peak appears with the increasing peak transmission, and the high- and low-frequency resonant slightly blue- and red-shifts, respectively. More importantly, the EIA-like effect is achieved, and the peak absorption rapidly increases from 25% to 50% when the coupling strength becomes weaker. Contrary to the absorption spectra shown in Fig. 4(b), the absorption peak slightly red-shifts. Therefore, the transmission and absorption spectra of the proposed metamaterial can be efficiently controlled by designing its metamolecule, which offers an effective way to manipulate resonant behavior in metamaterials.

In conclusion, we propose a single-layer planar metamaterial consisting of an array of two coupled R and D resonators. We have numerically demonstrated a classical analog of EIT and EIA in the metamaterial at optical frequencies. Given the occurrence of destructive interference in the far-field, the coupling of a radiative mode and a dark mode leads to a high-Q EIT-like transmission pass band showing a Fano-type asymmetric line shape. The dark mode excitation is very important to achieve EIT and EIA phenomena. The induced field distributions are utilized to understand resonance hybridization between

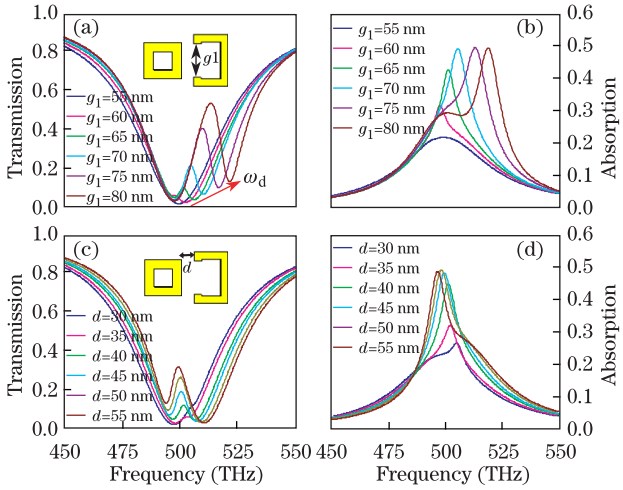

Fig. 4. (a) and (b) Transmission and absorption spectra of the CRR-SRR metamaterial with the distance d=40 nm for different split widths g_1; (c) and (d) transmission and absorption spectra of the CRR-SRR metamaterial with g_1=65 nm for different coupling distances d.

two elements for achieving the EIT effect in the planar metamaterial. Frequency detuning is easily controlled by adjusting the width of the split in one resonator and strongly affecting the interaction between the dark and radiative modes. In addition to the enhanced transmission in the case of the EIT effect, the near-field coupling of the bright mode to the dark mode results in a narrow peak of enhanced absorbance up to 2.5 times on top of the broad dipolar absorption feature. In particular, the coupling strength in the currently proposed metamaterial can easily modulate properties of the EIA phenomenon. Increasing loss of the dark resonator and decreasing the coupling strength can result in the EIA-like effect in the metamaterial. The spectral feature of metamaterials can be easily engineered using well-designed metamolecules. Therefore, the proposed metamaterials serve as promising candidates for many applications, such as in optical filters, sensing, slow light, and in nonlinear optics.

This work was supported by the National Natural Science Foundation of China (Nos. 61201083, 61275094, and U1231201), the Natural Science Foundation of Heilongjiang Province in China (No. LC201006), the China Postdoctoral Science Foundation (Nos. 2012M511171 and 2013T60487), the Special Foundation for Harbin Young Scientists (No. 2012RFLXG030), the Fundamental Research Funds for the Central Universities, and the 111 Project of the Harbin Engineering University (No. B13015).

References

1. N. I. Zheludev and Y. S. Kivshar, Nat. Mat. **11,** 917 (2012).
2. H. F. Ma and T. J. Cui, Nat. Comm. **1,** 124 (2010).
3. F. Falcone, T. Lopetegi, M. A. G. Laso, J. D. Baena, J. Bonache, M. Beruete, R. Marqués, F. Martín, and M. Sorolla, Phys. Rev. Lett. **93,** 197401 (2004).
4. V. A. Fedotov, P. L. Mladyonov, S. L. Prosvirnin, A. V. Rogacheva, Y. Chen, and N. I .Zheludev, Phys. Rev. Lett. **97,** 167401 (2006).
5. R. Singh, E. Plum, C. Menzel, C. Rockstuhl, A. K. Azad, R. A. Cheville, F. Lederer, W. Zhang, and N. I. Zheludev, Phys. Rev. B. **80,** 153104 (2009).
6. J. H. Shi, X. C. Liu, S. W. Yu, T. T. Lv, Z. Zhu, H. F. Ma, and T. J. Cui. Appl. Phys. Lett. **102,** 191905 (2013).
7. X. Li, S. Xiao, B. Cai, Q. He, T. J. Cui, and L. Zhou, Opt. Lett. **37,** 4940 (2012).
8. E. Plum, X. -X. Liu, V. A. Fedotov, Y. Chen, D. P. Tsai, and N. I. Zheludev, Phys. Rev. Lett. **102,** 113902 (2009).
9. R. Singh, E. Plum, W. L. Zhang, and N. I. Zheludev, Opt. Express **18,** 13425 (2010).
10. N. Yu, P. Genevet, M. A. Kats, F. Aieta, J. P. Tetienne, F. Capasso, and Z. Gaburro, Science **334,** 333 (2011).
11. X. Zhang, Z. Tian, W. Yue, J. Gu, S. Zhang, J. Han, and W. Zhang, Adv. Mater. **25,** 4567 (2013).
12. X. B. Yin, Z. L. Ye, J. Rho, Y. Wang, and X. Zhang, Science **339,** 1405 (2013).
13. H. T. Chen, W. J. Padilla, J. M. O. Zide, A. C. Gossard, A. J. Taylor, and R. D. Averitt, Nature **444,** 597 (2006).
14. Q. J. Du, J. S. Liu, and H. W. Yang, Chin. Opt. Lett. **9,** 110015 (2011).
15. R. Singh, X. C. Lu, J. Q. Gu, Z. Tian, and W. L. Zhang, J. Opt. **12,** 015101 (2010).
16. D. R. Chowdhury, R. Singh, M. Reiten, J. F. Zhou, A. J. Taylor, and J. F. O'Hara, Opt. Express **19,** 10679 (2011).
17. R. Singh, C. Rockstuhl, F. Lederer, and W. L. Zhang, Appl. Phys. Lett. **94,** 021116 (2009).
18. Y. Yang, R. Huang, L. Q. Cong, Z. H. Zhu, J. Q. Gu, Z. Tian, R. Singh, S. Zhang, J. G. Han, and W. L. Zhang, Appl. Phys. Lett. **98,** 121114 (2011).
19. R. Singh, C. Rockstuhl, and W. L. Zhang, Appl. Phys. Lett. **97,** 241108 (2010).
20. I. A. I. Al-Naib, R. Singh, C. Rockstuhl, F. Lederer, S. Delprat, D. Rocheleau, M. Chaker, T. Dzaki, and R. Morandotti, Appl. Phys. Lett. **101,** 071108 (2012).
21. R. Singh, I. A. I. Al-Naib, M. Koch, and W. L. Zhang, Opt. Express **18,** 13044 (2010).
22. D. R. Chowdhury, R. Singh, M. Reiten, H. T. Chen, A. J. Taylor, J. F. O'Hara, and A. K. Azad, Opt. Express **19,** 15817 (2011).
23. Z. Tian, R. Singh, J. G. Han, J. Q. Gu, Q. R. Xing, J. Wu, and W. L. Zhang, Opt. Lett. **35,** 3586 (2010).
24. V. A. Fedotov, M. Rose, S. L. Prosvirnin, N. Papasimakis, and N. I. Zheludev, Phys. Rev. Lett. **99,** 147401 (2007).
25. S. Zhang, D.A. Genov, Y. Wang, M. Liu, and X. Zhang, Phys. Rev. Lett. **101,** 047401 (2008).
26. N. Papasimakis, V. A. Fedotov, N. I. Zheludev, and S. L. Prosvirnin, Phys. Rev. Lett. **101,** 253903 (2008).
27. S. Y. Chiam, R. Singh, C. Rockstuhl, F. Lederer, W. L. Zhang, and A. A. Bettiol, Phys. Rev. B. **80,** 153103(2009).
28. N. Liu, L. Langguth, T. Weiss, J. Kästel, M. Fleischhauer, T. Pfau, and H. Giessen, Nat. Mater. **8,** 758 (2009).
29. C. Kurter, P. Tassin, L. Zhang, T. Koschny, A. P. Zhuravel, A. V. Ustinov, S. M. Anlage, and C. M. Soukoulis, Phys. Rev. Lett. **107,** 043901 (2011).
30. Z. Y. Li, Y. F. Ma, R. Huang, R. Singh, J. Q. Gu, Z. Tian, J. G. Han, and W. L. Zhang, Opt. Express **19,** 8912 (2011).
31. X. J. Liu, J. Q. Gu, R. Singh, Y. F. Ma, J. Zhu, Z. Tian, M. X. He, J. G. Han, and W. L. Zhang, Appl. Phys. Lett. **100,** 131101 (2012).
32. X. Q. Lu, J. H. Shi, R. Liu, and C. Y. Guan, Opt. Express **20,** 17581 (2012).
33. J. Q. Gu, R. Singh, X. J. Liu, X. Q. Zhang, Y. F. Ma, S. Zhang, S. A. Maier, Z. Tian, A. K. Azad, H. T. Chen, A. J. Taylor, J. G. Han, and W. L. Zhang, Nat. Comm. **3,** 1151 (2012).
34. L. Zhu, F. Y. Meng, J. H. Fu, Q. Wu, and J. Hua, Opt. Express **20,** 4494(2012).
35. L. Zhang, P. Tassin, T. Koschny, C. Kurter, S. M. Anlage, and C. M. Soukoulis, Appl. Phys. Lett. **97,** 241904 (2010).
36. X. Q. Zhang, Q. Li, W. Cao, J. Q. Gu, R. Singh, Z. Tian, J. G. Han, and W. L. Zhang, IEEE J. Select. Topics Quantum Electron. **19,** 8400707 (2013).
37. A. Yang, C. C. Yan, J. B. Tian, C. Wang, G. M. Li, and D. H. Zhang, Chin. Opt. Lett. **11,** 051602 (2013).
38. B. Luk'yanchuk, N. I. Zheludev, S. A. Maier, N. J. Halas, P. Nordlander, H. Giessen, and C. Chong, Nat. Mater. **9**, 707 (2010).
39. A. E. Miroshnichenko, S. Flach, and Y. S. Kivshar, Rev. Mod. Phys. **82,** 2257 (2010).
40. V. A. Fedotov, A. Tsiatmas, J. H. Shi, R. Buckingham, P. de Groot, Y. Chen, S. Wang, and N. I. Zheludev, Opt. Express **18,** 9015 (2010).
41. R. Singh, I. A. I. Al-Naib, M. Koch, and W. L. Zhang,

Opt. Express **19,** 6312 (2011).

42. Y. F. Ma, Z. Y. Li, Y. M. Yang, R. Huang, R. Singh, S. Zhang, J. Q. Gu, Z. Tian, J. G. Han, and W. L. Zhang, Opt. Mat. Express **1,** 391 (2011).
43. R. Singh, I. A. I. Al-Naib, Y. P. Yang, D. R. Chowdhury, W. Cao, C. Rockstuhl, T. Ozaki, R. Morandotti, and W. L. Zhang, Appl. Phys. Lett. **99,** 201107 (2011).
44. W. Cao, R. Singh, I. A. I. Al-Naib, M. X. He, A. J. Taylor, and W. L. Zhang, Opt. Lett. **37,** 3366 (2012).
45. J. H. Shi, Z. Zhu, H. F. Ma, W. X. Jiang, and T. J. Cui, J. Appl. Phys. **112,** 073522 (2012).
46. C. Wu, A. B. Khanikaev, R. Adato, N. Arju, A. A. Yanik, H. Altug, and G. Shvets, Nat. Mater. **11,** 69 (2012).
47. R. Liu, J. H. Shi, E. Plum, V. A. Fedotov, and N. I. Zheludev, Acta Phys. Sin. **61,** 154101 (2012).
48. J. Zhao, C. Zhang, P. V. Braun, and H. Giessen, Adv. Mat. **24,** OP247 (2012).
49. R. Taubert, M. Hentschel, J. Kästel, and H. Giessen, Nano Lett. **12,** 1367 (2012).
50. L. Verslegers, Z. Yu, Z. Ruan, P. B. Catrysse, and S. Fan, Phys. Rev. Lett. **108,** 083902 (2012).
51. P. Tassin, L. Zhang, R. K. Zhao, A. Jain, T. Koschny, and C. M. Soukoulis, Phys. Rev. Lett. **109,** 187401 (2012).
52. Y. Sun, W. Tan, L. Liang, H. T. Jiang, Z. G. Wang, F. Q. Liu, and H. Chen, Europhys. Lett. **98,** 64007 (2012).
53. Y. Lu, H. Xu, J. Y. Rhee, W. H. Jang, B. S. Ham, and Y. P. Lee, Phys. Rev. B **82,** 195112 (2010).
54. R. Singh, C. Rockstuhl, F. Lederer, and W. L. Zhang, Phys. Rev. B. **79,** 085111 (2009).
55. I. Al-Naib, R. Singh, M. Shalaby, T. Ozaki, and R. Morandotti, IEEE J. Select. Topics Quantum Electron. **19,** 8400807 (2013).
56. D. R. Chowdhury, R. Singh, A. J. Taylor, H. -T. Chen, and A. K. Azad, Appl. Phys. Lett. **102,** 011122 (2013).
57. X. Q. Zhang, Q. Li, W. Cao, W. S. Yue, J. Q. Gu, Z. Tian, J. G. Han, and W. L. Zhang, Chin. Opt. Lett. **9,** 110012 (2011).
58. J. H. Shi, R. Liu, B. Na, Y. Q. Xu, Z. Zhu, Y. K. Wang, H. F. Ma, and T. J. Cui, Appl. Phys. Lett. **103,** 071906 (2013).
59. J. Shao, J. Q. Li, J. Li, Y. K. Wang, Z. G. Dong, P. Chen, R. X. Wu, and Y. Zhai, Appl. Phys. Lett. **102**, 034106 (2013).
60. P. Tassin, L. Zhang, T. Koschny, E. N. Economou, and C. M. Soukoulis, Phys. Rev. Lett. **102,** 053901 (2009).
61. K. Aydin, I. M. Pryce, and H. A. Atwater, Opt. Express **18,** 13407 (2010).